SLAS Discovery 27 (2022) 167–174

Contents lists available at ScienceDirect

SLAS Discovery

journal homepage: www.elsevier.com/locate/slasd

Full Length Article

Mass spectrometry-based proteomics of 3D cell culture: A useful tool to validate culture of spheroids and organoids

Thayna Mendonca Avelino[a,b], Marta García-Arévalo[a], Felipe Rafael Torres[a], Marieli Mariano Goncalves Dias[a,c], Romenia Ramos Domingues[a], Murilo de Carvalho[a], Matheus de Castro Fonseca[a], Vanessa Kiraly Thomaz Rodrigues[a], Adriana Franco Paes Leme[a], Ana Carolina Migliorini Figueira[a,b,c,*]

[a] National Center of Research in Energy and Materials (CNPEM), National Laboratory of Bioscience (LNBio)
[b] State University of Campinas (UNICAMP), Department of Pharmacology Science
[c] State University of Campinas (UNICAMP), Department of Molecular and Functional Biology

ARTICLE INFO

Keywords:
Spheroids
Obesity
Adipogenesis
Mass spectrometry
Proteomics

ABSTRACT

Worldwide obesity, defined as abnormal or excessive fat accumulation that may result in different comorbidities, is considered a pandemic condition that has nearly tripled in the last 45 years. Most studies on obesity use animal models or adipocyte monolayer cell culture to investigate adipose tissue. However, besides monolayer cell culture approaches do not fully recapitulate the physiology of living organisms, there is a growing need to reduce or replace animals in research. In this context, the development of 3D self-organized structures has provided models that better reproduce the in vitro aspects of the in vivo physiology in comparison to traditional monolayer cell culture.

Besides, recent advances in omics technologies have allowed us to characterize these cultures at the proteome, metabolome, transcription factor, DNA-binding and transcriptomic levels. These two combined approaches, 3D culture and omics, have provided more realistic data about determined conditions. Thereby, here we focused on the development of an obesity study pipeline including proteomic analysis to validate adipocyte-derived spheroids. Through the combination of collected mass spectrometry data from differentiated 3T3-L1 spheroids and from murine white adipose tissue (WAT), we identified 1732 proteins in both samples. By using a comprehensive proteomic analysis, we observed that the in vitro 3D culture of differentiated adipocytes shares important molecular pathways with the WAT, including expression of proteins involved in central metabolic process of the adipose tissue. Together, our results show a combination of an orthogonal method and an image-based analysis that constitutes a useful pipeline to be applied in 3D adipocyte culture.

Introduction

Overweight and obesity are defined as abnormal or excessive fat accumulation, an issue that has grown to epidemic proportions causing the death of nearly 4 million people per year due to health complications, according to the global burden of disease [1]. To find solutions for obesity, the biomedical researchers have been exploring the development of adipocyte cell culture and adipose tissue models [2] to understand biological mechanisms with the aim of designing interventions to achieve and maintain healthy metabolism and body weight. Instead of using animals, most of the studies are performed in vitro using adipocytes, being the mouse 3T3-L1 cell line the most common model for this purpose [6-8].

For many years researchers have been using animal models to answer important scientific questions aiming to understand obesity and overweight [2,3]. The use of animal models could be often costly, time-consuming and present scientific limitations such as poor relevance to human biology [4]. The proposed Principles of Human Experimental Technique promulgated the 3Rs of Replacement, Reduction and Refinement [5] in science. Since then, researchers have been developing new methods to substitute animal models which can also fill the gaps inherent to them mainly when knowledge must be translated to human physiology. Currently, cell monolayer is widely used, however, they do not represent tissue morphology, organization and physiology; to bring in vitro experiments closer to those performed with animals, several models of 3D cell culture have been developed [6-8]. The 3D cell culture is an in vitro self-organized and stimulus-sensitive representation of an in vivo tissue being more realistic than cultures in monolayer [9]. The adipocyte spheroids and organoids have been developed to help substitute the animal use in obesity research. Therefore, it is crucial

* Corresponding author.
E-mail address: ana.figueira@lnbio.cnpem.br (A.C.M. Figueira).

https://doi.org/10.1016/j.slasd.2021.10.013

Available online 27 October 2021

to investigate and characterize these models in comparison with the well-established animal models used in metabolic research and preclinical testing.

Moreover, recent advances in omics technologies, such as mass spectrometry (MS), have become an extensively applied method for 3D cultures characterization. The development of methodologies and improvements in the resolution and sensitivity of MS instruments have allowed it to address a variety of biological questions [10,11]. Here we present the development of an obesity study pipeline including proteomic analysis to validate adipocyte-derived spheroids. Our results indicate MS-based proteomics as a method to validate spheroidal 3D cell culture of mouse 3T3-L1 cells to study adipose tissue and its molecular pathways, which correlates with white adipose tissue (WAT).

Methods

3T3-L1 cell culture and differentiation

3T3-L1 mouse preadipocytes were obtained from American Type Culture Collection (ATCC). 3T3-L1 mouse preadipocytes (passage 10-15) were cultured in high glucose (4.5 g/L) Dulbecco's Modified Eagle Medium supplemented with 10% calf serum and 100 U/mL penicillin 100 mg/mL streptomycin at 5% CO_2 and 37 ˚C and harvested before reaching 70% confluence for spheroid assemble. After assembled, the spheroids were differentiated with the use of the induction medium for 48h composed of DMEM, 10% FBS, 1% w/v antibiotics (penicillin and streptomycin), 1 µM dexamethasone, 1 µg/mL of insulin and 0.5 mM of 3-isobutyl-1-methylxanthine (IBMX). After the induction period, medium was aspirated and the maintenance medium composed of DMEM, 10% FBS, 1% w/v antibiotics, 1 µg/mL insulin was added. The maintenance medium was changed every 48 hours until reaching 14 days of differentiation.

Spheroid assemble

Based on the afore described method [8], cells after reaching a 70% confluence were counted and the nanomagnetic particles NanoShuttle ™-PL (Greiner) were added in the proportion of 1 uL for each $1x10^4$ cells. After magnetization, $1,5x10^4$ cells were added to a 96-well culture plate (Greiner Bio-One 655970 - 96 well microplate, PS, well with F/chimney bottom, cell-repellent surface, clear, sterile), (Fig.1). For spheroids formation, a device with 96 magnetic cylinders (Greiner Bio-One 655830) was positioned below the culture plate and the cells remained 24 hours incubated with magnets and kept in a humid incubator at 37 ˚C and 5 % CO_2.

Animal model

Male C57BL/6J mice were purchased from Model Organisms Laboratory (LOM) mouse facility at LNBio/CNPEM (Campinas, SP, Brazil). Mice were weaned with 21 days old and were maintained at 22 ± 1 ˚C on a 12 hours light-dark cycle, with free access to food and water. They were fed a chow diet (Nuvilab CR1) for 12 weeks. The composition of the diet is as follows: crude protein, 220 g/kg; fat, 50 g/kg; carbohydrate, 600 g/kg; crude fiber, 70 g/kg; neutral detergent fiber 200 g/kg (20%), ash, 90 g/kg (9%); energy density, 3860 kcal/kg; calories from protein, 22%; calories from fat, 5%; and calories from carbohydrate, 60%.

At the age of 17 weeks, mice were euthanized in fed state and the perigonadal white adipose tissue (WAT) pads were dissected, washed in PBS and immediately frozen with liquid nitrogen. Later, they were stored at –80 ˚C until use. The Ethical Committee of CNPEM/LNBio "Comissão de Ética no Uso de Animais" (CEUA-CNPEM) specifically reviewed and approved this study (approval identification 61). The protocols were performed following the guidelines for ethical conduct in the care and use of animals established by the Brazilian Society of Laboratory Animal Science (SBCAL/COBEA). Animals were treated humanely and with regard to alleviate suffering.

Spheroid viability and size

On the day of assemble (day 0) and days 2, 4, 6, 8, 10, 12 and 14; 12 spheroids were collected per day in order to measure the cell viability through ATP production. The ATP was quantified using a CellTiter-Glo® 3D Cell Viability Assay (Promega, cat. G9681) following the manufacturer's instructions; the luminescence was recorded in a Glow Max Plate Reader (Promega). The spheroids diameter was measured every 2 days. The images were captured with Operetta High Content Imaging System (Perkin Elmer, Waltham, MA, USA) and quantified using Harmony Software (Perkin Elmer).

Microscopy

The lipid droplets and the nuclei were stained after spheroids were fixed for 1 hour in 4% formalin and washed 3 times in PBS. The LipidSpot (Biotium; cat. Number 70065-T) lipid marker probe and the DAPI (Biotium; cat. Number 40043) were added according with manufacturer's instructions. After staining with the fluorescent probes, the images were obtained using a TCS SP8 (Leica) confocal microscope.

Sample preparation for X-ray microtomography

The 3T3-L1 spheroids were fixed in 4% formalin for 1 hour at room temperature, contrasted with 0.4% osmium solution, and then dehydrated in ethanol baths (70%, 80%, 90%, 95% and 100%). After dehydration, samples were clarified in two xylol baths (30 minutes each) and included in paraplast Plus® (sigma; cat. Number P3683-1KG). The included samples were mounted on a stub in the rotation stage.

X-ray microtomography

Briefly the 3T3-L1 spheroids mounted on a stub were submitted to micro tomography, the images were acquired at the Synchrotron National Light Laboratory (LNLS), on the beamline dedicated to X-ray micro tomography (IMX). More than 2000 X-ray transmission images were obtained by rotating the sample in 360 degrees around a fixed rotation axis, in uniformly spaced angular steps, to produce a stack of synograms that were later computationally transformed into a 3D density map sample electronics [12].

The 3D reconstructed data obtained on the IMX beamline were processed using the Avizo Fire 9.4 software (https://www.fei.com/software/avizo-for-materials- science/). A median filter was applied to all images to remove noise and allow segmentation and quantification of the image. After filtering, an interactive threshold was applied, in order to separate the signal from the noise. The reconstructed and filtered 3D image was visualized using the 3D rendering function.

Proteomics

Proteolytic digestion

All samples, WAT, non-differentiated (ND) and differentiated 3T3-L1 spheroids (WA), were submitted to the same protocol of protein extraction and trypsin digestion. Briefly, the samples were homogenized with 8 M urea, 2 M thiourea in 30 mM Tris-HCl pH 8.5, containing 1 mM EDTA, and 1 mM PMSF. The proteins were quantified by Bradford method [13] and an aliquot containing 10 µg of proteins was submitted to reduction. Proteins were reduced with 5 mM dithiothreitol (DTT) for 25 minutes at 56 ˚C and alkylated with 14 mM iodoacetamide (IAA) for 30 minutes at room temperature in the dark. The remaining IAA was removed by the addition of excess DTT. To reduce the final concentration of urea to 1 M, the mixtures were diluted with 50 mM ammonium bicarbonate buffer. Proteins were digested with trypsin (1:50, w/w) for 18 hours at 37˚C, and then 1% formic acid (v/v) was added to stop the digestion. The tryptic peptides were desalted with C18 stage tips [14].

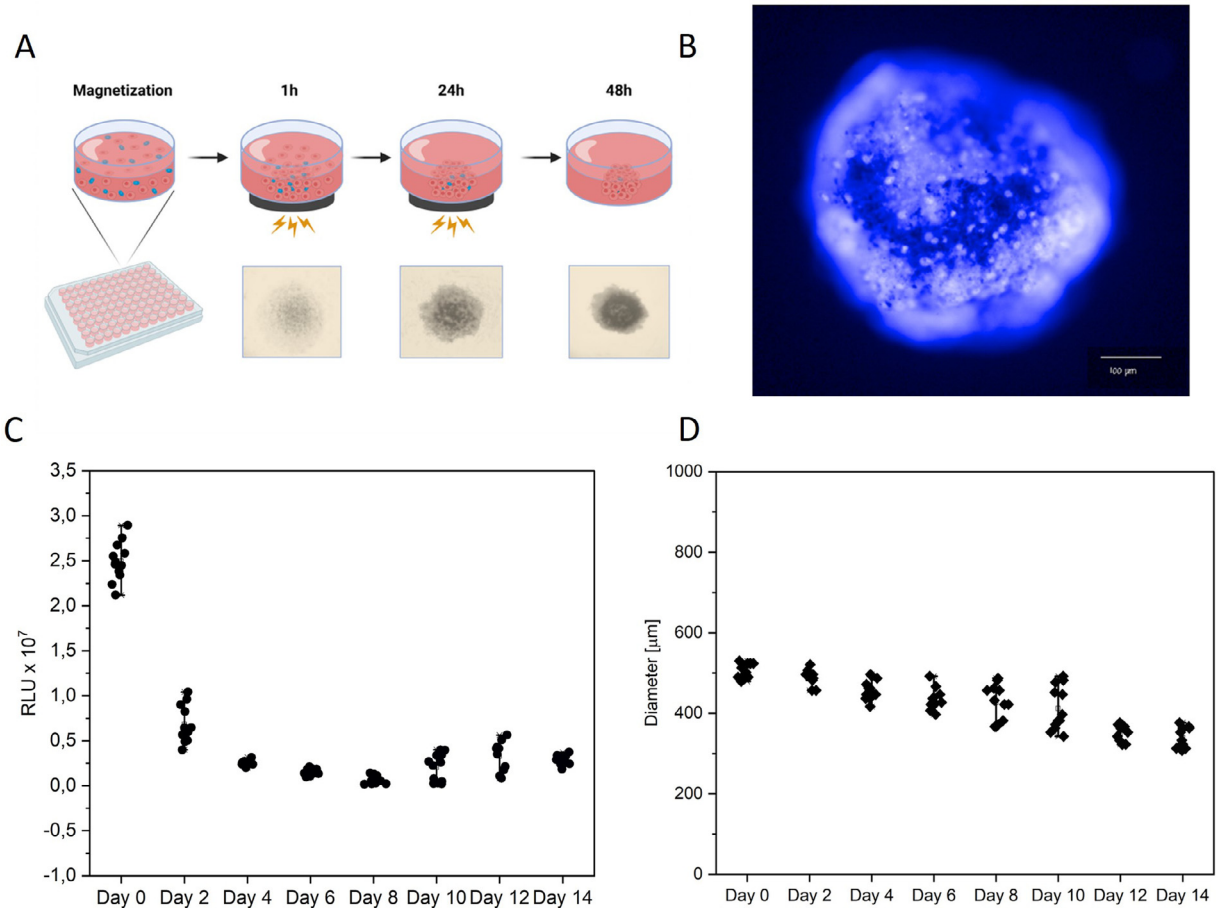

Fig. 1. A. Scheme of Scaffold-free generation of spheroids and Phase-contrast image of spheroids, after magnetization the plate was incubated at 37 °C in a humidified chamber for 1 day to allow for magnetic assembly of pre-adipocytes into spheroids. The resultant spheroids were then differentiated for applications. Spheroids were maintained in base media showed no appreciable change in size after 2 weeks of observation. B. fluorescence image of spheroid after assembled, stained with DAPI, measurements realized showed sphericity around 1. C. ATP measurements of spheroids for 14 days. The ATP was quantified with CellTiter-Glo®, luminescence was recorded with one spheroid per well. The dot plots represent the luminescence mean ± SD (n= 12 spheroids per day), the statistical test ANOVA two way, (adjusted p-value < 0.05) indicate that the day of the spheroids were make (day 0) and the day 2 were significantly different from the measurement of other days, from day 4 the spheroids appear to stabilize the ATP production. D. Measurement of spheroids diameter during 14 days, the measurement was performed with n= 12 spheroids/day in an automatized microscopy. The statistical test, ANOVA two way, (adjusted p-value < 0.05) indicate no significance variation for 10 days.

To avoid bias during measurements, all data collection was randomized using the R (v3.4.0) environment.

LC-MS/MS analysis

The peptide mixtures (2.0ml) were analyzed using an LTQ Orbitrap Velos (Thermo Fisher Scientific) mass spectrometer coupled to nanoflow liquid chromatography on an EASY-nLC system (Proxeon Biosystems) with a Proxeon nanoelectrospray ion source. Peptides were separated in a 2 to 35% acetonitrile gradient in 0.1% formic acid, using a PicoFrit analytical column (20 cm × ID 75,5 μm particle size, New Objective), at a flow rate of 300 nL/min over 175 minutes, as previously described [15].

Proteomic data analysis

Raw data were processed using MaxQuant v1.5.8 software [27], and MS/MS spectra were searched against the Mus musculus UniProt database (released in December, 2020, 63,724 sequences, and 28,586,808 residues) using the Andromeda search engine [28]. A tolerance of 10 ppm was considered for precursor ions, and 1 Da for-fragment ions, with a maximum of two missed cleavages. A fixed modification of carbamidomethylation of cysteine and variable modifications of methionine oxidation and protein N-terminal acetylation were considered. A 1% false discovery rate (FDR) was set for both protein and peptide identifications. Protein quantification was performed using the LFQ algorithm, with a minimal ratio count of 1 and a window of 2 minutes for matching between runs. Data were processed in Perseus v1.6.7.0 software, excluding reverse sequences and those identified "only by site" entries. Protein abundance was calculated based on the normalized spectrum intensity (LFQ intensity) and was log2-transformed. The significance was assessed using Student's t-test (P-value < 0.05). For data visualization, Volcano plot was performed with fold-change (FC) and p-value threshold value of 2.0 and 0.05, respectively, using the software Metaboanalyst v 5.0.

Results

Spheroids are stable for at least 14 days

Cultured 3T3-L1 pre-adipocytes were assembled in spheroids according to the already proposed methodology [16]. Spheroids were set up with $1.5x10^4$ 3T3-L1 cells and magnetized for 24 hours resulting in a spherical 3D structure (Fig. 1-A, B). After magnetization, the spheroids were kept in culture for 14 days in basal medium and evaluated for their stability and viability. ATP production and diameter were checked every two days, and the data obtained showed that until day 2 the culture seems to be in a period of high metabolic demand, probably because of

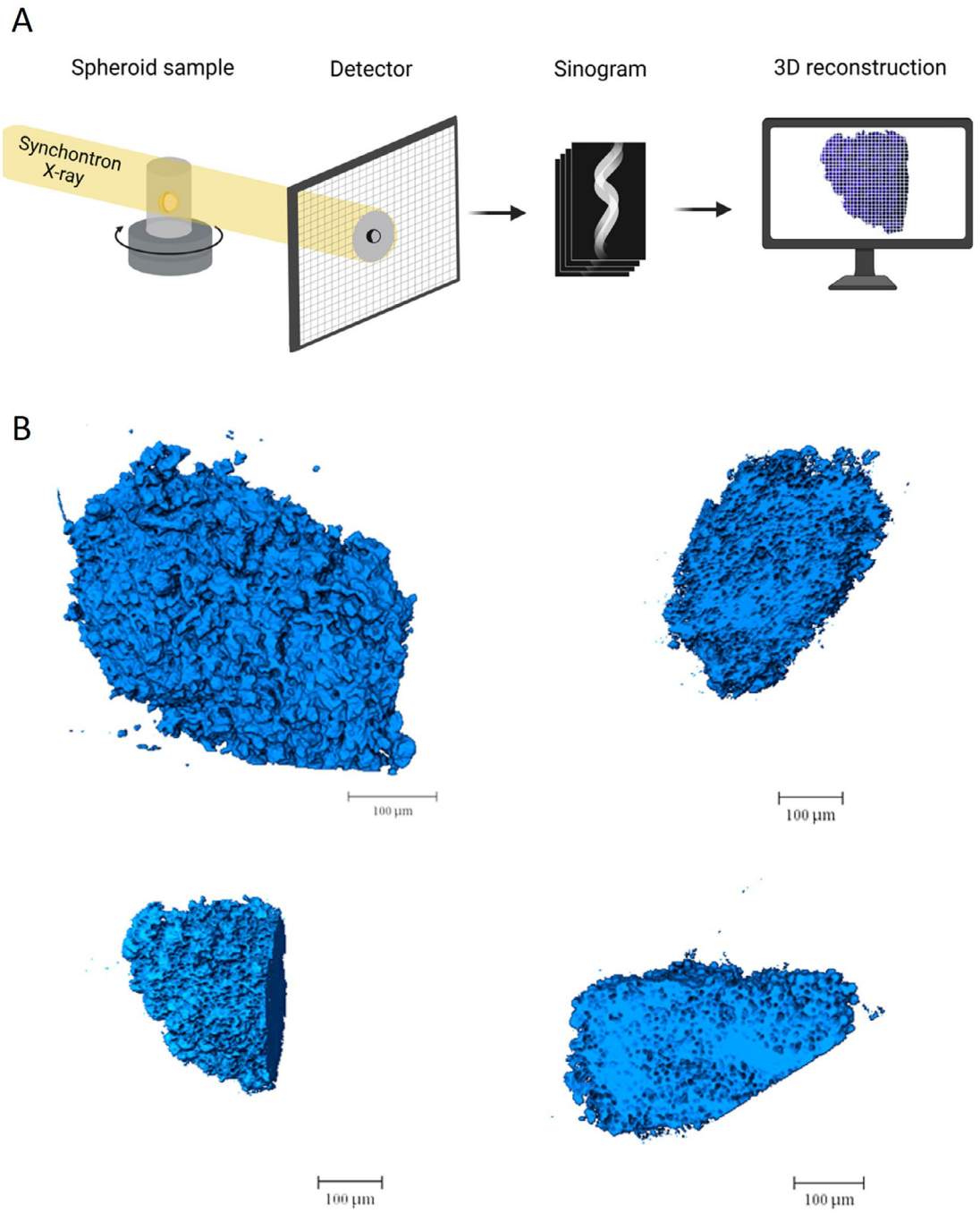

Fig. 2. A. Scheme of data acquisition on IMX beam line. The fixed samples were stained and mounted in a stub and exposed to synchrotron x-ray. Images were acquired and recorded as a sinograms; all data were computationally processed and reconstructed using a specific 3D reconstruct software (Avizo) B. X-Ray Micro-tomography characterization of pre-adipocyte spheroids. The image of a whole spheroid is depicted in the superior left, at superior right and inferior left are the reconstructed images of two different cross sections and at inferior right is the center of the spheroid, showing no lack of cell in its nuclei. The spheroids size quantification demonstrated that they retain an elliptical format, with an average diameter of 200 um and 500µm long.

the change of the type of culture from monolayer to 3D. From day 4 on, the spheroids reached stability on ATP production (Fig. 1-C), suggesting that cell viability was kept.

Additionally, spheroid diameter (Fig. 1-D) was measured concomitantly to ATP quantification, exhibiting low variation until day 12, when the quantification indicated a reduction of the diameter, without cell death as founded in ATP quantification. Finally, to characterize the spheroid shape, the confocal fluorescence measurement indicated that spheroids are compact and well-formed, presenting sphericity around 1(Fig. 1-B).

Micro-tomography revealed uniform and reproducible 3T3-L1 spheroids

To access the internal structure and morphology, the spheroids (N=24) were submitted to high-resolution synchrotron-based X-ray microtomography (IMX). Spheroids, processed as indicated in method section, were mounted on a stub in the rotation stage for data acquisition (Fig. 2-A).

The 3D reconstructed data obtained on the IMX demonstrated that 3T3-L1 cells formed uniform and stable spheroids, as can be observed through the morphological details on X-ray microtomography images.

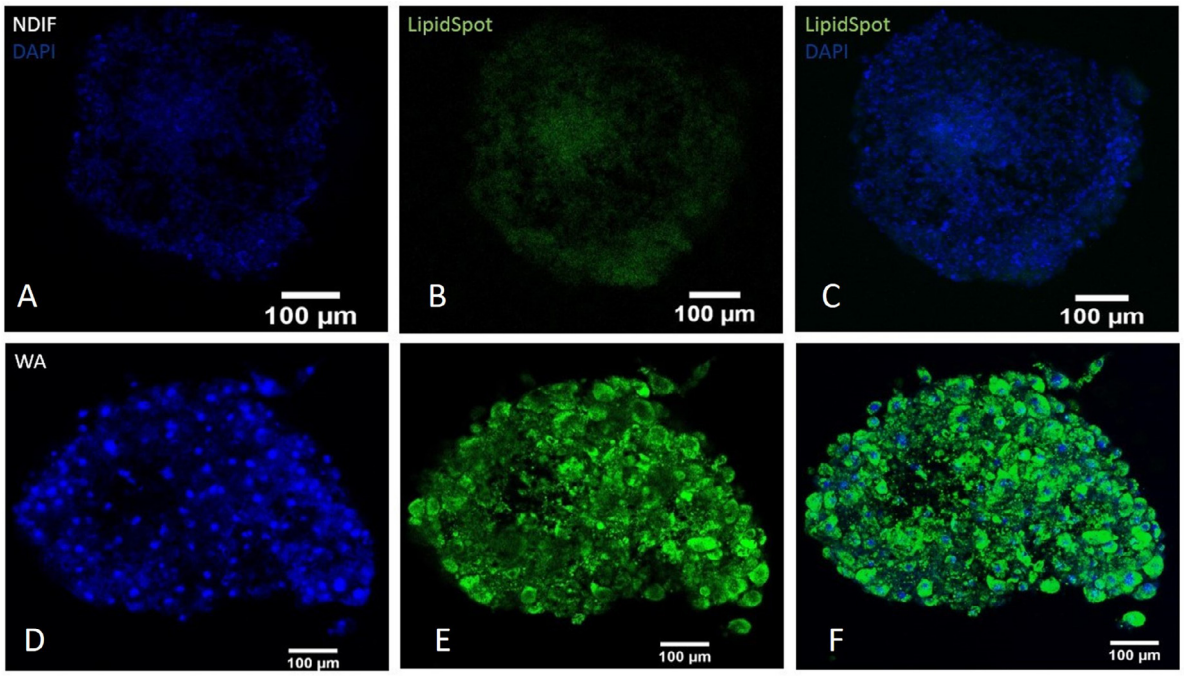

Fig. 3. In panel, spheroids no differentiated in the superior line (NDIF, A, B, C) and differentiated spheroids in the inferior line (WA, D, E, F). The cell's nucleus were stained with DAPI (A, D), lipid droplets were stained with LipidSpot (B, E) and both staining were superposed (C, F). Almost the whole space of adipocytes is occupied by lipid droplets after 14 days exposed to differentiated cocktail (WA) when compared with undifferentiated condition (NDIF). Confocal laser scan microscopy was applied to detect DAPI and LipidSpot.

Cross section images showed the absence of deformed nuclei, which indicates that formed spheroids do not exhibit necrotic centers. Also, it was observed that spheroids present external shape of an elliptical form featuring well-adhered cells and average size of 500 µm (Fig. 2B).

3T3-L1 spheroids developed lipid droplets on cells characterizing mature adipocytes

To produce adipocyte-derived spheroids, 3T3-L1-assembled spheroids were differentiated for 14 days. After differentiated, spheroids were stained with LipidSpot (Fig.3) to assess the increase of lipid content in the adipocyte cytoplasm. Confocal images of differentiated (WA) and undifferentiated (NDIF) spheroids (Fig. 3) showed an increase in lipid droplets in spheroids treated with differentiation medium (WA), when compared to NDIF spheroids. The presence of lipid droplets indicated a mature state of adipocytes.

Proteomics of adipose tissue spheroids demonstrated similarity to mouse adipose tissue

As an orthogonal method to investigate molecular similarity between murine white adipose tissue (WAT) and differentiated 3T3-L1-derived spheroids (WA), we characterized the global proteome of WA (n=24) and perigonadal WAT from mice (n=3).

Tissue dissected from mice and differentiated spheroids from three independent experiments were lysate to extract the proteins. The extraction had a protein average yield of 1,5µg/µl and 10µg of protein lysate of each sample (pool of spheroids and perigonadal WAT) were submitted to proteolytic digestion (Fig. 4-A). After proteolytic digestion, the peptide mixture was analyzed using an LTQ Orbitrap Velos (Thermo Fisher Scientific) mass spectrometer coupled to nanoflow liquid chromatography on an EASY-nLC system (Proxeon Biosystems) with a Proxeon nanoelectrospray ion source. The proteomes of WAT and WA spheroids were analyzed using quantitative MS and label-free protein quantitation (LFQ intensity) to compare the relative abundance of proteins.

The data shows that for WA, 646 proteins were confidently identified. For the WAT dataset, 1083 proteins were quantified. The proteomic data analysis identified 536 common and exclusive proteins from WA spheroids and WAT (Fig. 4-A). Paired Student's t test (P value < 0.05) indicated 110 proteins that were preferentially expressed in WA, and 547 in WAT. The relatively small number of protein expression identified exclusively in WA spheroids reflects their biological similarity to WAT, and the higher number of identified proteins in WAT reflects the complexity of a real tissue extracted from an organism. As expected, non-differentiated spheroids were very different in terms of found proteins in WA and WAT (Supplementary Figure 1 – FS1).

Biological replicates from WA and WAT were combined to investigate proteomic changes. The Volcano plot, in Fig. 4-B, shows the up and downregulated proteins, in which 63 proteins were upregulated and 43 downregulated in WAT. Moreover, the 13 proteins with major difference of expression between the groups are named in the graph (Fig. 4-B), most of them are associated with fatty acid metabolism, mitochondrial activity, and energy expenditure. On the other hand, 101 proteins (Supplementary material – Table 1) did not present significant difference in expression profile between the groups, indicating that half of the expressed proteins in spheroids and in mouse tissue are the same and presented the same expression rates, which is a strong validation of how our spheroids can mimic the mouse organism.

Enrichment analysis of biological processes of differentiated adipose spheroids

Functional enrichment analysis for the combined up- and downregulated proteins was performed to analyze biological processes. Enriched processes of WA compared to WAT are shown in Figure 5. This classification system uses information on protein sequence to assign a gene to an ontology group based on the Gene Ontology (GO) terms http://www.geneontology.org/.

The results obtained in functional enrichment featured that 7 of 15 processes are shared between WA and WAT. In general, for similar bio-

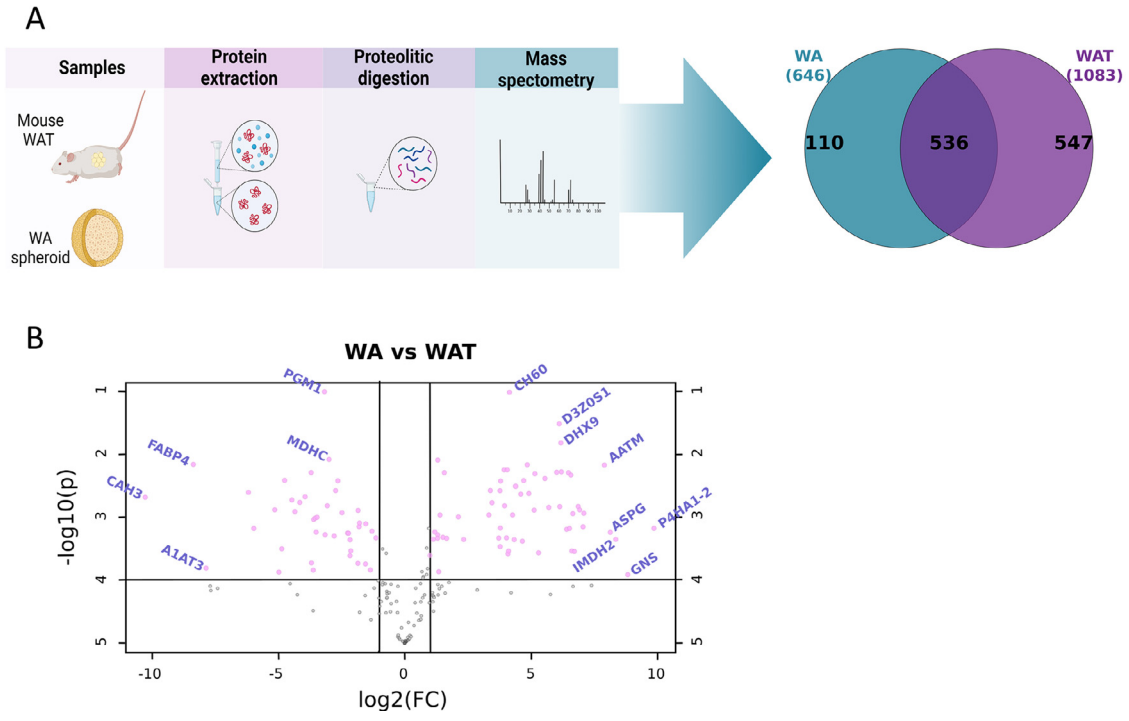

Fig. 4. A. Pipeline of mass spectrometry-based proteomics of adipose spheroids and white adipose tissue. The samples (WAT or WA spheroids) were submitted to protein extraction; proteolytic digestion followed by MS analysis. Venn diagram of identified proteins, WA and WAT share 536 common proteins, WA have 110 exclusive proteins and WAT 547 proteins. B. Volcano plots for experimental comparison of WA X WAT in which abundance ratio (Log2) is plotted against the p-value (−log10). There are 63 upregulated proteins and 43 downregulated proteins indicated in plot (adjusted p-value < 0.05), in the right side in pink are the proteins up regulated in WA and in left the proteins up regulated in WAT, the proteins with major expression difference are named in the graph. The proteins plotted in grey color (101) did not present expression profile differences between the groups, that means the similarity between the groups.

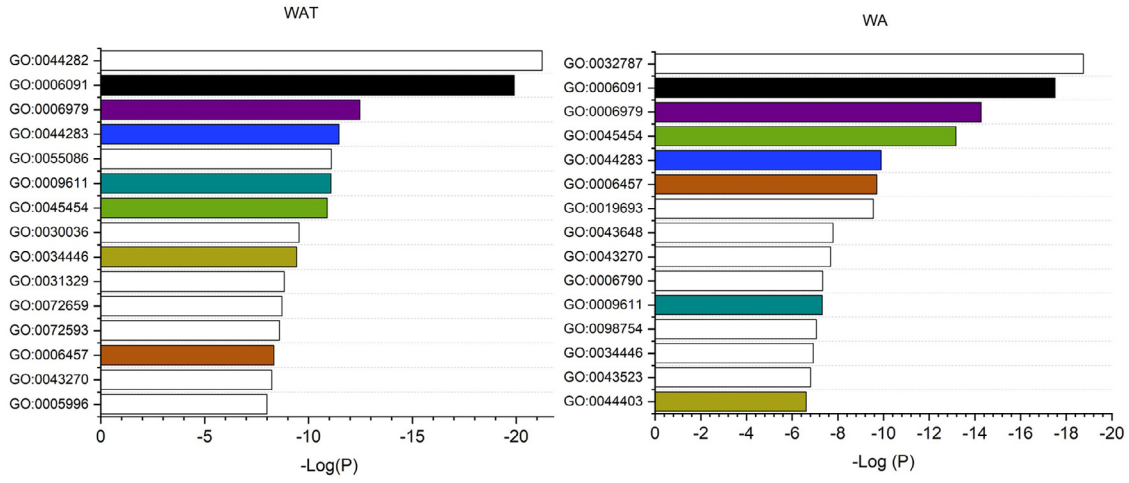

Fig. 5. Functional enrichment analysis of murine WAT (left) and WA spheroids (right). A combined list of significantly up- and downregulated proteins was used for analysis, and an adjusted p-value <0.05 was considered statistically significant. Enrichment analysis for GO biological processes was performed using METASCAPE. Bar colors indicate groups of selected processes that appear in the two groups. The biological processes names and IDs, GO:0043270 Positive regulation of ion transport; GO:0006457 Protein folding; GO:0072593 Reactive oxygen species metabolic process; GO:0072659 Protein localization to plasma membrane; GO:0031329 Regulation of cellular catabolic process; GO:0034446 Substrate adhesion-dependent cell spreading; GO:0030036 Actin cytoskeleton organization; GO:0045454 Cell redox homeostasis; GO:0009611 Response to wounding; GO:0055086 Nucleobase-containing small molecule metabolic process ; GO:0044283 Small molecule biosynthetic process; GO:0006979 Response to oxidative stress; GO:0006091 Generation of precursor metabolites and energy; GO:0044282 Small molecule catabolic process; GO:0032787 Monocarboxylic acid metabolic process; GO:0019693 Ribose phosphate metabolic process; GO:0043648 Dicarboxylic acid metabolic process; GO:0006790 Sulfur compound metabolic process; GO:0043270 Positive regulation of ion transport; GO:0043523 Regulation of neuron apoptotic process; GO:0034446 Substrate adhesion-dependent cell spreading; GO:0098754 Detoxification.

logical processes found enriched in WAT and WA, the most significantly ones are related to generation of precursor metabolites and energy. The analysis revealed the regulation of various metabolic processes in WA with a central role in adipose tissue, being the response to oxidative stress (represented in purple in Fig. 4) one of the top enriched. Moreover, other metabolic processes were identified in which the most significant were monocarboxylic catabolic acid process and oxoacid metabolic process.

Regarding the differentially enriched metabolic processes between WA and WAT, WA was enriched in carbohydrate metabolism, detoxification, symbiotic interaction, and neuron apoptotic process, while WAT was enriched in plasma lipoprotein particle levels, catabolism, cytoskeleton and mitochondrion organization, and small molecule metabolism, including ROS metabolism. However, despite some of those processes not being identical, they presented some similarities when grouped in a higher order. As an example, protein regulation-related processes, which were presented as protein-binding regulation in WA and as protein stabilizing/membrane-anchoring processing WAT; or carbohydrate metabolism-related process that was more detailed in WA and was restricted to monosaccharide metabolic process in WAT. Additionally, functional enrichment analysis was performed to evaluate the biological processes of non-differentiated (ND) spheroids, comparing ND, WA and WAT. From these group, only one process (GO:0006457 Protein folding) was shared (Supplementary material – FS1), the low similarity probably is related to metabolic characteristics of a non-differentiated cells comparing to an adipocyte. In summary, WA and WAT share 7 significantly enriched biological processes indicated by functional analysis.

Discussion

The worldwide pandemic of obesity demands efforts to understand the mechanisms involved in metabolic unbalance caused by overweight being the adipose tissue a central player in obesity treatment and control. Furthermore, the advent of 3D cultures made possible the development of disease and tissue models that can be used to substitute or, at least, to contribute with studies using traditional animal models in research. Moreover, these 3D cultures have been considered more realistic and reduce the average number of animals in experimentation. Some studies demonstrated that 3T3-L1 spheroids could be valuable models to investigate obesity and adipogenesis [17-20], contributing with new evidences in biological mechanisms of these conditions. Even though adipose spheroids present morphological similarities to adipose tissue, their application as an ally or substitute of animal models depends on their capacity of recapitulation other physiological characteristics of this tissue. Our data show that differentiated 3T3-L1-derived spheroids produced stable and uniform cultures as shown in details by microtomography. To validate the spheroid model, we proposed a proteomics analysis of WA spheroid in comparison to murine WAT. This evaluation provided novel insights about this type of 3D culture and the potential differences found between this model and the tissue from a living organism. In a quantitative proteomics approach, a total of 1726 unique proteins were identified in both samples. WA and WAT share 536 proteins, representing 83% of the total identified proteins in WA spheroids. This data indicates a high similarity rate between 3D WA model and the tissue dissected from the animal. The proteins recovery for WAT after submitted to protein extraction presented superior yield in comparison with proteins recovery in WA, certainly because the complexity of a tissue, which cannot be totally reproduced in spheroids and organoids.

Recently, some studies reported the proteomic profile of 3T3-L1 adipocytes in monolayer [21,22]. Similar to data obtained from proteomics in monolayer, our protein enrichment analysis data revealed various processes associated with the regulation of metabolism, including those involved in adipogenesis and fatty acid metabolism. Both processes are fundamental for the physiology of the tissue that we propose to mimic.

The enrichment analysis of biological processes revealed important pathways shared between WA and WAT. One of them was the "response to the oxidative stress" associated with preadipocyte proliferation increase, adipocyte differentiation, and the size of mature adipocytes [23-26]. In obesity, this biological process is related to a several health disfunctions [26], showing once again the great resemblance of our 3D model with the murine WAT itself. Another enriched process, "generation of precursor metabolites and energy" is on the top of the enriched processes listed in both models. It represents an important pathway for adipocytes involved in the regulation of energy consumption and expenditure. Also, this pathway was associated to energy expenditure during exercise and as a diabetic marker [29,30]. All these results indicate that the functional enrichment data was an important tool to identify which biological processes are present in both animal and 3D cell culture model. With this data we exhibit that it is possible to use the 3D models more assertively, with focus on proteins present in keys biological pathways.

In summary, here we proposed a model to validate 3D cultures comparing them to a model organism. Our findings demonstrate that differentiated 3T3-L1 spheroids recapitulate important in vivo properties of murine WAT and provide a framework for future investigations to decipher underlying mechanisms and test therapeutic targets to manage or treat diseases associated with adipose tissue like obesity.

Declaration of Competing Interest

The authors declare that the research was conducted in the absence of any commercial or financial relationships that could be construed as potential conflict of interest.

This article is being reproduced in print post-publication in a sponsored print collection for distribution. The company sponsoring the print collection was not involved in the editorial selection or review of this article.

Acknowledgments

We thank Model Organisms Laboratory (LOM) at LNBio/CNPEM for providing animal facility. We acknowledge the 3D Cell Culture Laboratory (LC3D), the Mass Spectrometry facility (MAS) and the Spectroscopy and Calorimetry facility (LEC) of the Brazilian Biosciences National Laboratory (LNBio), CNPEM, Campinas, Brazil, for providing support on spheroid culture, on LC-MS/MS analysis, and in luminescence measurements. We also thank UVX facility of the Brazilian Synchrotron Light Laboratory (LNLS) and beamline staff for the assistance during the experiments [Proposal number 20180615]. All these facilities are part of the Brazilian Center for Research in Energy and Materials (CNPEM), a private non-profit organization under the supervision of the Brazilian Ministry for Science, Technology, and Innovations (MCTI). This work was supported by the “Fundação de Amparo à Pesquisa do Estado de São Paulo” (FAPESP) [process # 2019/14465-0, 2019/10274-7]; “Conselho Nacional de Desenvolvimento Científico e Tecnológico” (CNPq) [process # 302567/2017-5]; “Coordenação de Aperfeiçoamento de Pessoal de Nível Superior” (CAPES) [8887.373113/2019-00], and CNPEM.

Supplementary materials

Supplementary material associated with this article can be found, in the online version, at doi:10.1016/j.slasd.2021.10.013.

References

[1] World Health Organization. Noncommunicable diseases progress monitor, 2017. WHO https://www. who.int/nmh/publications/ncd-progress-monitor-2017/en/ (2017).
[2] Speakman J, Hambly C, Mitchell S, Król E. Animal models of obesity. Obes Rev 2007;8(1):55–61 2007 MarSuppl00319. x. doi:10.1111/j.1467-789X.

[3] Lutz TA, Woods SC. Overview of animal models of obesity. Curr Protoc Pharmacol 2012 ;Chapter 5: Unit5.61. doi:10.1002/0471141755.ph0561s58.
[4] National Centre for Replacement. Refinement and Reduction of Animals in Research 2021. Available at https://www.nc3rs.org.uk/the-3rs accessed.
[5] Russell WMS, Burch RL. The Principles of Humane Experimental Technique. London: Methuen & Co Ltd; 1959.
[6] Klingelhutz AJ, Gourronc FA, Chaly A, Wadkins DA, Burand AJ, Markan KR, Idiga SO, Wu M, Potthoff MJ, Ankrum JA. Scaffold-free generation of uniform adipose spheroids for metabolism research and drug discovery. Sci Rep 2018;8(1):523. doi:10.1038/s41598-017-19024-z.
[7] Unser AM, Tian Y, Xie Y. Opportunities and challenges in three-dimensional brown adipogenesis of stem cells. Biotechnol Adv 2015;33(6):962–79 Pt 1Epub 2015 Jul 29. doi:10.1016/j.biotechadv.2015.07.005.
[8] DAQUINAG Alexes C, e SOUZA, Glauco R, e KOLONIN, Mikhail G. Adipose Tissue Engineering in Three-Dimensional Levitation Tissue Culture System Based on Magnetic Nanoparticles. Tissue Engineering Part C: Methods 2013.
[9] Edmondson R, Broglie JJ, Adcock AF, Yang L. Three-dimensional cell culture systems and their applications in drug discovery and cell-based biosensors. Assay Drug Dev Technol 2014;12(4):207–18 2014 May.573. doi:10.1089/adt.
[10] Migisha Ntwali PV, Heo Chae Eun, Han Jong Yoon, Chae Soo Yeon, Kim Minji, Vu Hung M, Kim Min-Sik, Kim Hugh I. Mass spectrometry-based proteomics of single cells and organoids: The new generation of cancer research. TrAC Trends in Analytical Chemistry 2020;130:116005 ISSN 0165-9936. doi:10.1016/j.trac.2020.116005.
[11] Gonneaud A, Asselin C, Boudreau F, Boisvert FM. Phenotypic Analysis of Organoids by Proteomics. Proteomics 2017;17(20) 2017 OctEpub. doi:10.1002/pmic.201700023.
[12] Fonseca MdC, Araujo BHS, Dias CSB, et al. High-resolution synchrotron-based X-ray microtomography as a tool to unveil the three-dimensional neuronal architecture of the brain. Sci Rep 2018;8:12074. doi:10.1038/s41598-018-30501-x.
[13] Bradford MM. A rapid and sensitive method for the quantitation of microgram quantities of protein utilizing the principle of protein-dye binding. Anal Biochem 1976;72:248–54. doi:10.1006/abio.1976.9999.
[14] Rappsilber J, Mann M, Ishihama Y. Protocol for micro-purification, enrichment, pre-fractionation and storage of peptides for proteomics using StageTips. Nat Protoc 2007;2:1896–906. doi:10.1038/nprot.2007.261.
[15] Carnielli CM, Macedo CCS, De Rossi T, Granato DC, Rivera C, Domingues RR, Pauletti BA, Yokoo S, Heberle H, Busso-Lopes AF, Cervigne NK, Sawazaki-Calone I, Meirelles GV, Marchi FA, Telles GP, Minghim R, Ribeiro ACP, Brandão TB, de Castro G Jr González-Arriagada WA, Gomes A, Penteado F, Santos-Silva AR, Lopes MA, Rodrigues PC, Sundquist E, Salo T, da Silva SD, Alaoui-Jamali MA, Graner E, Fox JW, Coletta RD. Paes Leme AF. Combining discovery and targeted proteomics reveals a prognostic signature in oral cancer. Nat Commun 2018 Sep 5;9(1):3598. doi:10.1038/s41467-018-05696-2.
[16] Souza GR, Molina JR, Raphael RM, Ozawa MG, Stark DJ, Levin CS, Bronk LF, Ananta JS, Mandelin J, Georgescu MM, Bankson JA, Gelovani JG, Killian TC, Arap W, Pasqualini R. Three-dimensional tissue culture based on magnetic cell levitation. Nat Nanotechnol 2010 Mar 14;5(4):291–6 2010 AprEpub. doi:10.1038/nnano.2010.23.
[17] Fischbach C, Spruss T, Weiser B, Neubauer M, Becker C, Hacker M, Göpferich A, Blunk T. Generation of mature fat pads in vitro and in vivo utilizing 3-D long-term culture of 3T3-L1 preadipocytes. Exp Cell Res 2004 Oct 15;300(1):54–64. doi:10.1016/j.yexcr.2004.05.036.
[18] Turner PA, Tang Y, Weiss SJ, Janorkar AV. Three-dimensional spheroid cell model of in vitro adipocyte inflammation. Tissue Eng Part A 2015 Apr 22;21(11-12):1837–47 2015 JunEpub. doi:10.1089/ten.TEA.2014.0531.
[19] Daquinag AC, Souza GR, Kolonin MG. Adipose tissue engineering in three-dimensional levitation tissue culture system based on magnetic nanoparticles. Tissue Eng Part C Methods 2012 Nov 2;19(5):336–44 2013 MayEpub. doi:10.1089/ten.TEC.2012.0198.
[20] Turner PA, Garrett MR, Didion SP, Janorkar AV. Spheroid Culture System Confers Differentiated Transcriptome Profile and Functional Advantage to 3T3-L1 Adipocytes. Ann Biomed Eng 2018;46(5):772–87 2018 May-yEpub. doi:10.1007/s10439-018-1993.
[21] Chan H, Bhide KP, Vaidyam A, Hedrick V, Sobreira TJP, Sors TG, Grant RW, Aryal UK. Proteomic Analysis of 3T3-L1 Adipocytes Treated with Insulin and TNF-α. Proteomes. 2019 Oct 20;7(4):35. doi: 10.3390/proteomes7040035.
[22] Choi S, Goswami N, Schmidt F. Comparative Proteomic Profiling of 3T3-L1 Adipocyte Differentiation Using SILAC Quantification. J Proteome Res 2020;19(12):4884–900 Epub 2020 Oct 8. doi:10.1021/acs.jproteome.0c00475.
[23] Furukawa S, Fujita T, Shimabukuro M, et al. Increased oxidative stress in obesity and its impact on metabolic syndrome. J Clin Invest 2004;114:1752–61.
[24] Lee H, Lee YJ, Choi H, et al. Reactive oxygen species facilitate adipocyte differentiation by accelerating mitotic clonal expansion. J Biol Chem 2009;284:10601–9.
[25] Higuchi M, Dusting GJ, Peshavariya H, et al. Differentiation of human adipose-derived stem cells into fat involves reactive oxygen species and Forkhead box O1 mediated upregulation of antioxidant enzymes. Stem Cells Dev 2013;22:878–88.
[26] Manna P, Obesity Jain SK, Stress Oxidative. Adipose Tissue Dysfunction, and the Associated Health Risks: Causes and Therapeutic Strategies. Metab Syndr Relat Disord 2015;13(10):423–44. doi:10.1089/met.2015.0095.
[27] Cox J, Mann M. MaxQuant enables high peptide identification rates, individualized p.p.b.-range mass accuracies and proteome-wide protein quantification. Nat Biotechnol 2008;26(12):1367–72 2008 DecEpub. doi:10.1038/nbt.1511.
[28] Cox J, Neuhauser N, Michalski A, Scheltema RA, Olsen JV, Mann M. Andromeda: a peptide search engine integrated into the MaxQuant environment. J Proteome Res 2011;10(4):1794–805 Epub 2011 Feb 22. doi:10.1021/pr101065j.
[29] Li H, Li X, Guo J, et al. Identification of biomarkers and mechanisms of diabetic cardiomyopathy using microarray data. Cardiol J 2020;27(6):807–16. doi:10.5603/CJ.a2018.0113.
[30] Aldiss P, Lewis JE, Lupini I, et al. Exercise Training in Obese Rats Does Not Induce Browning at Thermoneutrality and Induces a Muscle-Like Signature in Brown Adipose Tissue. Front Endocrinol (Lausanne) 2020;11:97 2020Published. doi:10.3389/fendo.2020.00097.